

Statistical Mechanics of Semiflexible Polymer Chains from a new Generating Function

Marcelo Marucho^{a)}, Leonardo Loureiro^{b)} and Gustavo A. Carri^{c)}

The Maurice Morton Institute of Polymer Science,

The University of Akron, Akron, OH 44325-3909, USA.

Abstract

In this paper, we present a new approach to the Kratky-Porod Model (KP) of semiflexible polymers. Our solution to the model is based on the definition of a generating function which we use to study the statistical mechanics of semiflexible polymer chains. Specifically, we derive mathematical expressions for the characteristic function, the polymer propagator and the mean square end-to-end distance from the generating function. These expressions are valid for polymers with any number of segments and degree of rigidity. Furthermore, they capture the limits of fully flexible and stiff polymers exactly. In between, a smooth and approximate crossover behavior is predicted. The most important contribution of this paper is the expression of the polymer propagator which is written in a very simple and insightful way. It is given in terms of the exact polymer propagator of the Random Flight Model multiplied by an exponential that takes into account the stiffness of the polymer backbone.

Electronic address:^{a)}marucho@polymer.uakron.edu

Electronic address:^{b)}lla2@uakron.edu

Electronic address:^{c)}carri@polymer.uakron.edu

To whom any correspondence should be addressed

I. INTRODUCTION

Since the ground-breaking ideas by Kratky and Porod in 1949,¹ theoretical studies of semiflexible polymers based on the KP model have been abundant. In this model, the polymer chain displays resistance to bending deformations. This resistance is modeled using a free energy that penalizes bending the polymer backbone. The free energy depends on parameters (elastic constants) that are a consequence of many short-range monomer-monomer interactions. Explicitly, for the continuous version of the KP model² (called the Wormlike Chain Model, WCM) the free energy is

$$H = \frac{\epsilon}{2} \int_0^L ds \left(\frac{\partial \mathbf{R}}{\partial s} \right)^2, \quad (1)$$

where $\mathbf{R}(s)$ is the vectorial field that represents the polymer chain, s is the arc of length parameter, L is the contour length of the polymer and ϵ is the bending modulus. In addition, the local inextensibility constraint $|d\mathbf{R}(s)/ds| = 1$ must be satisfied.

As a consequence of the bending rigidity, a semiflexible chain is characterized by a persistence length (proportional to the bending modulus) such that, if the length scale is shorter than the persistence length, then the chain behaves like a rod while, if the length scale is larger than the persistence length, then the chain is governed by the configurational entropy that favors the random-walk conformations.

The local inextensibility constraint has not allowed researchers to find an exact solution to the model. Indeed, the constraint $|d\mathbf{R}(s)/ds| = 1$ is written using a Dirac delta distribution in infinite dimensions. Depending on how the constraint is written, $|d\mathbf{R}(s)/ds| = 1$ or $(d\mathbf{R}(s)/ds)^2 = 1$, we get an Edwards Hamiltonian that is non-analytic or non-linear, respectively. Consequently, there is no exact solution of this model at present. However, a few properties like the first few moments of the distribution of the end-to-end distance^{2,3} are known exactly.

Indeed, many researchers have addressed the Kratky-Porod and other models of semiflexible polymers with the purpose of understanding the statistical behavior of this kind of polymers. Among the many theoretical treatments of semiflexible polymers, let us start by mentioning two very important contributions done in the 1950s: the work by Daniels⁴ who developed expansions of the polymer propagator for a semiflexible polymer in inverse powers of the number of segments and the classic paper by Benoit and Doty⁵ who obtained

the exact expression for the average end-to-end distance squared and radius of gyration. During the following two decades, the field of statistical mechanics of semiflexible polymers saw a substantial growth thanks to the seminal contributions of many researchers. For example, Fixman and Kovacs developed a modified Gaussian model for stiff polymer chains under an external field (external force).⁶ In this approach, they computed an approximate distribution for the bond vectors from which they were able to compute the partition function and average end-to-end vector. An alternative approach was proposed by Harris and Hearst⁷ who developed a distribution for the continuous model from which they were able to compute the two-point correlation function and, consequently, the mean-square end-to-end distance and radius of gyration. A reformulation of the KP model using field-theoretic methods was developed by Saitô and coworkers² who computed exactly different averages of the end-to-end distance and tangent-tangent correlation function. In addition, Gobush and coworkers⁸ developed an asymptotic expression for the polymer propagator in inverse powers of the number of segments and, Yamakawa and Stockmayer⁹ addressed the first order corrections to the end-to-end distance squared and second virial coefficient due to excluded volume interactions. Semiflexible polymers were also extensively studied by Freed¹⁰ who employed field-theoretic methods to study their statistical behavior. A few years later, he developed a modified Gaussian distribution approximation to the continuous version of the KP model¹¹ which has been re-derived using different mathematical methods by Lagowski and coworkers,¹² and Winkler and coworkers.¹³ Similar results were obtained by Zhao and coworkers¹⁴ who also studied the effect of an external field. Field-theoretic methods have also been used by Bhattacharjee and Muthukumar¹⁵ who employed the Edwards-Singh self-consistent approach to obtain an effective Gaussian Hamiltonian from which they computed the average end-to-end distance squared.

In recent years, the advent of new experimental methods that have allowed researchers to manipulate single molecules has generated new momentum in the area of statistical mechanics of semiflexible polymers.¹⁶ Indeed, new analytical approaches to semiflexible polymers have been developed by Marko and Siggia, and Kroy and Frey¹⁷ who derived the force versus elongation behavior predicted by the WCM, Hansen and Podgornik¹⁸ who developed a non-perturbative $1/d$ expansion (d being the dimension of the embedding space), Wilhem and Frey¹⁹ who computed the polymer propagator for polymers with large bending rigidities and Winkler²⁰ who computed the same quantity for any value of the stiffness of the poly-

mer backbone using the Maximum Entropy Principle. Finally, it is worth mentioning one alternative approach to semiflexible polymers (Dirac chains) developed by Kholodenko.²¹

The aforementioned extensive list of approximate treatments of the KP model, though not exhaustive, does show two major trends. On the one hand, many studies computed different statistical properties as perturbative corrections to the rod-like and flexible limits. One example of this statement is the seminal paper by Gobush *et al.* where the polymer propagator was computed as a perturbation expansion with respect to the Gaussian chain model (see Eqs. (22) and (23) in Ref. 8). On the other hand, many researchers have targeted a few physical properties of the KP model and optimized the approximations to capture these properties exactly or very accurately. Two examples of this statement are: the paper by Bawendi and Freed,¹¹ who optimized their treatment of the KP model (continuous version) to reproduce the bond-bond projection expectation value exactly and obtained a modified Gaussian distribution for the end-to-end distance (see Eq. (13) in Ref. 11), and the paper by Winkler *et al.*¹³ who used a very fundamental concept, the Maximum Entropy Principle, to compute different ensemble averages and correlation functions (the constraints used to optimize the use of the Maximum Entropy Principle are given by Eqs. (3.25) to (3.28) in Ref. 13). These observations lead naturally to the following two questions . Firstly, we should ask “why do we need so many different approximations to solve the same model?” and, secondly, “can we find one approximation capable of predicting all the statistical properties of the model in such a way that corrections to these results can be computed in a systematic and perturbative fashion ?”. Observe that the answer to the latter is affirmative for the problem of a single flexible polymer with excluded volume interaction.²²

In this paper we address the second question. In other words, we address the KP model with the purpose of finding one “ground” state capable of reproducing all the statistical properties of the model approximately. Furthermore, we require that our “ground” state captures all the statistical properties of the rod-like and flexible limits exactly and respects the local, not global, inextensibility constraint. In the crossover region, the solution is not exact but, we require that it displays the correct physical features as described by other treatments of the model and, moreover, it should be amenable to systematic and controlled corrections calculated in a perturbative manner around the “ground” state. In this first paper, we set the Fixman parameter to zero and leave the excluded volume problem for a future publication.

The most important prediction of this calculation is the polymer propagator which turns out to be proportional to the polymer propagator of the Random Flight Model²³ multiplied by an exponential arising from the stiffness of the polymer backbone described by the parameter α (see text for details),

$$P(R) \sim P_{RFM}(R) \exp[R^2/2\alpha n^2],$$

where n is the number of segments and R is the end-to-end distance. The mathematical simplicity of this expression makes it a very good candidate for the development of a perturbative treatment of the KP model.

This paper is organized as follows. In section II, we propose a generating function and obtain an approximate analytical expression for it. This section also contains the only approximation of our calculation. Afterward, we use the generating function to calculate the characteristic function, mean squared end-to-end distance and polymer propagator of the model. In Section III we discuss the results of our calculations which are valid for any value of the stiffness of the polymer backbone and length of the polymer chain. For the purpose of making our presentation more balanced and objective, we compare our results with those obtained by other researchers. Section IV contains the conclusions of our work. The details of some mathematical calculations are presented in the appendix.

II. THEORY

A. Review of the Kratky-Porod Model and Evaluation of the new Generating Function

Let us consider a polymer chain as a set of n bond vectors $(\mathbf{u}_0, \mathbf{u}_1, \dots, \mathbf{u}_{n-1})$ connected in a sequential manner. Furthermore, let us assume that the length of each bond vector is l_k (=Kuhn length) and that pairs of consecutive bond vectors try to be parallel to each other. This orientational interaction is modeled with a Boltzmann weight given by the following expression^{6,15}

$$\exp\left(-\frac{\epsilon}{2l_k^2 k_B T} \sum_{k=0}^{n-2} (\mathbf{u}_{k+1} - \mathbf{u}_k)^2\right), \quad (2)$$

where ϵ and $k_B T$ are the bending modulus and thermal energy, respectively. In addition, we take into account the local inextensibility constraint with the following term²

$$\prod_{i=0}^{n-1} \delta \left\{ \frac{(\mathbf{u}_i)^2}{l_k^2} - 1 \right\}. \quad (3)$$

Equations (2) and (3) define the KP model completely and all the statistical properties of the model such as the characteristic function, single chain structure factor and other correlation functions, probability distributions like the polymer propagator and their moments can be calculated. The evaluation of these statistical properties can be easily done using the following generating function

$$C(\{\Psi_{kjp}\}) \equiv \left\langle \exp \left(\sum_{k=0}^{n-1} \mathbf{u}_k \cdot \Psi_{kjp} \right) \right\rangle, \quad (4)$$

where Ψ_{kjp} is

$$\Psi_{kjp} \equiv \mathbf{J}_k + i\mathbf{q} \cdot [\Theta(k-j) - \Theta(k-p)]. \quad (5)$$

This definition shows that Ψ_{kjp} is an auxiliary tensor. It represents a standard external source consisting of two terms: the first one, (\mathbf{J}_k) , represents a dipolar coupling with the k -th bond vector and, the second one, (\mathbf{q}) , is also a dipolar coupling that is non-zero only when the k -th bond vector is between the j -th and p -th ones. The $\Theta(z)$ function is the Heaviside step function.²⁴

If the generating function given by Eq.(4) is known, then all the aforementioned statistical properties can be obtained from it by differentiation with respect to \mathbf{J}_k and/or by assigning specific values to \mathbf{J}_k . For example, the characteristic function is $C(\{i\mathbf{q} \cdot [\Theta(k-j) - \Theta(k-p)]\})$ from which the polymer propagator is computed as the inverse Fourier transform of $C(\{i\mathbf{q}\})$, the tangent-tangent correlation function, $\langle \mathbf{u}_j \cdot \mathbf{u}_k \rangle$, is computed as the second derivative with respect to \mathbf{J}_j and \mathbf{J}_k which has to be evaluated at $\mathbf{J}_0 = \mathbf{J}_1 = \dots = \mathbf{J}_{n-1} = 0$. Other statistical quantities can also be computed easily.

Consequently, our first step is to evaluate $C(\{\Psi_{kjp}\})$ whose explicit form is

$$C(\{\Psi_{kjp}\}) = \frac{1}{z} \int \left[\prod_{i=0}^{n-1} d\mathbf{u}_i \delta \left\{ \frac{(\mathbf{u}_i)^2}{l_k^2} - 1 \right\} \right] \exp \left\{ -\frac{\epsilon}{2l_k^2 k_B T} \sum_{k=0}^{n-2} (\mathbf{u}_{k+1} - \mathbf{u}_k)^2 + \sum_{k=0}^{n-1} \mathbf{u}_k \cdot \Psi_{kjp} \right\}, \quad (6)$$

where z is defined such that $C(\{\mathbf{0}_{kjp}\}) = 1$. After writing the delta distributions in Eq.(6) in terms of their Fourier representations,²⁵ a Hubbard-Stratanovich transformation²⁶ is needed in order to avoid dealing with the quadratic term in \mathbf{u}_k arising from the exponential representation of the delta distributions. As a result, we get

$$C(\{\Psi_{kjp}\}) = \frac{1}{z} \int \left[\prod_{i=0}^{n-1} d\mathbf{u}_i d\lambda_i d\Phi_i \right] \exp \left(-\frac{\epsilon}{2l_k^2 k_B T} \sum_{k=0}^{n-2} (\mathbf{u}_{k+1} - \mathbf{u}_k)^2 - \frac{3}{2} \sum_{k=0}^{n-1} \left[\ln \lambda_k + i \frac{2}{3} \lambda_k \right] \right. \\ \left. + \sum_{k=0}^{n-1} \mathbf{u}_k \cdot \left(\Psi_{kjp} - i \frac{\Phi_k}{l_k} \right) - \frac{i}{4} \sum_{k=0}^{n-1} \frac{\Phi_k^2}{\lambda_k} \right), \quad (7)$$

where λ_k and Φ_k are dummy variables arising from the Fourier representation of the delta and the Hubbard-Stratanovich transformation, respectively. Observe that after redefining $\Psi_{kjp} l_k \rightarrow \Psi_{kjp}$ and $\mathbf{u}_k / l_k \rightarrow \mathbf{u}_k$, the dependence of Eq.(7) on the Kuhn length goes away.

We now proceed to compute the integrals over λ_k and \mathbf{u}_k . The λ_k -integrals are straightforward, the result is

$$\int \left[\prod_{i=0}^{n-1} d\lambda_i \right] \exp \left(-\frac{i}{4} \sum_{k=0}^{n-1} \frac{\Phi_k^2}{\lambda_k} - \frac{3}{2} \sum_{k=0}^{n-1} \left[\ln \lambda_k + i \frac{2}{3} \lambda_k \right] \right) \sim \prod_{i=0}^{n-1} \frac{\sin[(\Phi_i \cdot \Phi_i)^{\frac{1}{2}}]}{(\Phi_i \cdot \Phi_i)^{\frac{1}{2}}}, \quad (8)$$

where a constant prefactor independent of Φ_i has been neglected because of the definition of z in Eq.(6).

The \mathbf{u}_k -integrals are exactly doable using saddle point which is given by the following expression

$$\mathbf{u}_k = \mathbf{u}_0 - \frac{k_B T}{\epsilon} \sum_{m=0}^{k-1} (\Psi_{mjp} - i\Phi_m) (k - m), \quad (9)$$

where the following constrain must be fulfilled

$$\sum_{m=0}^{n-1} (\Phi_m + i\Psi_{mjp}) = 0. \quad (10)$$

Replacing Eqs.(8) and (9) into Eq.(7), and expressing the constraint as a delta distribution in the exponential representation, the generating function takes the form

$$C(\{\Psi_{kjp}\}) = \frac{1}{z} \int d\mathbf{u} \left\{ \int \left[\prod_{j=0}^{n-1} d\Phi_j \right] \exp \left[\sum_{j=0}^{n-1} \ln \left(\frac{\sin(|\Phi_j|)}{(|\Phi_j|)} \right) \right. \right. \\ \left. \left. - \frac{\kappa n}{2} \sum_{k=0}^{n-1} \sum_{s=0}^{n-1} (\Phi_k + i\Psi_{kjp}) K_{k,s} (\Phi_s + i\Psi_{sjp}) - i \sum_{s=0}^{n-1} \mathbf{u} \cdot (\Phi_s + i\Psi_{sjp}) \right] \right\}, \quad (11)$$

where the kernel $K_{k,s}$ and the parameter κ are defined as

$$K_{k,s} \equiv \left[1 - \frac{k}{n} - \frac{\Theta(s-k)}{n} (s-k) \right] \quad \text{and} \quad \kappa \equiv \frac{k_B T}{\epsilon}. \quad (12)$$

We refer the reader to Appendix A for some mathematical details of this part of the calculation.

The last step involves the evaluation of the Φ_j -integrals. Observe that this part of the calculation is not exactly doable thus, we approximate it as follows. First, we assume that, for a fixed value of s or k , the element of $K_{k,s}$ that contributes the most to the integral is the diagonal one. Thus, we approximate $K_{k,s}$ by its diagonal elements. The contributions arising from non-diagonal elements will be treated in a future publication. We also perform a pre-averaging approximation. Consequently, the kernel $K_{k,s}$ becomes

$$K_{k,s} \simeq \left\langle 1 - \frac{k}{n} \right\rangle \delta_{ks} = \frac{1}{2} \left(1 + \frac{1}{n} \right) \delta_{ks}, \quad (13)$$

This is the only approximation of our work. In the next section, we will show that this approximation captures the flexible (Random Flight Model) and rod-like limits exactly when $\kappa \rightarrow \infty$ and $\kappa \rightarrow 0$, respectively. This approximation also provides a very good crossover behavior for intermediate values of the parameter κ .

Equation (13) transforms the integrand of the \mathbf{u} -integral into

$$I_\Phi = \prod_{s=1}^{n-1} \int d\Phi_s \frac{\sin(|\Phi_s|)}{|\Phi_s|} \exp \left[-i\mathbf{u} \cdot (\Phi_s + i\Psi_{sjp}) - \frac{\alpha n}{2} (\Phi_s + i\Psi_{sjp})^2 \right], \quad (14)$$

where, for the purpose of simplicity, we have introduced a new parameter $\alpha \equiv \frac{1}{2} \left(1 + \frac{1}{n}\right) \kappa$.

Finally, replacing Eq.(14) in Eq.(11) we obtain the most general expression of the generating function $C(\{\Psi_{kjp}\})$. In the next section we evaluate some physical properties of the KP model using this generating function.

B. Characteristic Function and the Mean Square End-to-End Distance

Let us start by computing the characteristic function. For this purpose, we make $\Psi = i\mathbf{q}$ in Eq.(11) where \mathbf{q} is the scattering wave vector. Then, the characteristic function and the mean square end-to-end distance can be calculated. The Φ -integration takes the form

$$I_\Phi = \prod_{j=0}^{n-1} \int_0^\infty d\Phi \int_{-1}^1 d(\cos(\theta)) \int_0^{2\pi} d\varphi \sin(\Phi) \Phi \exp \left[-\frac{\alpha n}{2} (\Phi^2 + q^2) + i\mathbf{q} \cdot \mathbf{u} + \alpha n \mathbf{q} \cdot \Phi - i\mathbf{u} \cdot \Phi \right], \quad (15)$$

whose calculation is straightforward. Choosing θ to be the angle between the vectors \mathbf{u} and Φ , and θ_q the angle between \mathbf{q} and Φ , then the solution to the φ -integral is $2\pi I_0(\alpha n \Phi q |\sin(\theta) \sin(\theta_q)|)$ where $I_0(x)$ is the Bessel function of second class.²⁷ Hence, the angular integral, I_Ω , reads

$$I_\Omega = 2\pi \int_{-1}^1 d(\cos(\theta)) \exp [(-iu\Phi + \alpha n \Phi q \cos(\theta_q)) \cos(\theta)] I_0(\alpha n \Phi q |\sin(\theta) \sin(\theta_q)|) = 4\pi \frac{\sin \left(\Phi \sqrt{(\mathbf{u} + i\alpha n \mathbf{q})^2} \right)}{\Phi \sqrt{(\mathbf{u} + i\alpha n \mathbf{q})^2}}. \quad (16)$$

When we replace this expression into Eq.(15) we obtain the following form for I_Φ

$$I_\Phi = 4\pi \int_0^\infty d\Phi \sin(\Phi) \frac{\sin \left(\Phi \sqrt{(\mathbf{u} + i\alpha n \mathbf{q})^2} \right)}{\sqrt{(\mathbf{u} + i\alpha n \mathbf{q})^2}} \exp \left(-\frac{\alpha n}{2} (\Phi^2 + q^2) + i\mathbf{q} \cdot \mathbf{u} \right). \quad (17)$$

The solution of this integral is

$$= 4\pi \sqrt{\frac{\pi}{2\alpha n}} \frac{\sinh\left(\frac{1}{\alpha n}\sqrt{(\mathbf{u} + i\alpha n\mathbf{q})^2}\right)}{\sqrt{(\mathbf{u} + i\alpha n\mathbf{q})^2}} \exp\left(-\frac{1}{2\alpha n} - \frac{(\mathbf{u} + i\alpha n\mathbf{q})^2}{2\alpha n} + i\mathbf{q} \cdot \mathbf{u} - \frac{\alpha n}{2}\mathbf{q}^2\right). \quad (18)$$

Consequently, the characteristic function can be written as follows

$$C(q) = \frac{2\pi}{N} \left[4\pi \sqrt{\frac{\pi}{2\alpha n}} \right]^n \int_0^\infty du \int_{-1}^1 d(\cos(\theta)) \left[\frac{\sinh\left(\frac{1}{\alpha n}\sqrt{(\mathbf{u} + i\alpha n\mathbf{q})^2}\right)}{\sqrt{(\mathbf{u} + i\alpha n\mathbf{q})^2}} \right]^n u^2 \exp\left(-\frac{u^2}{2\alpha}\right), \quad (19)$$

where N is the norm which is defined in such a way that $C(0) = 1$.

In the limit of $\alpha \rightarrow \infty$, Eq.(19) approaches the asymptotic limit given by the formula

$$C_{\alpha \rightarrow \infty}(q) \sim \left[\frac{\sin(q)}{q} \right]^n, \quad (20)$$

which is the characteristic function of the Random Flight Model.²⁸

On the other hand, if $\alpha \rightarrow 0$,

$$C_{\alpha \rightarrow 0}(q) \sim \int_0^\infty du \int d\Omega u^{2-n} \exp\left(-\frac{u^2}{2\alpha} + iq n \cos(\theta)\right) \sinh^n(u/\alpha n) \sim \frac{\sin(qn)}{qn}, \quad (21)$$

and the Rod-like limit is recovered.²⁹

An expression for the entire range of values of α is obtained from Eq.(19). The first step is to compute the integral over the angles, that is

$$C_\Omega(q) = 2\pi \int_{-1}^1 d(\cos(\theta)) \left[\frac{\sinh\left(\frac{1}{\alpha n}\sqrt{(\mathbf{u} + i\alpha n\mathbf{q})^2}\right)}{\sqrt{(\mathbf{u} + i\alpha n\mathbf{q})^2}} \right]^n, \quad (22)$$

A variable transformation $v^2 = (u^2 - (\alpha n q)^2 + 2iu\alpha n q \cos(\theta))$ allows us to rewrite $C_\Omega(q)$

as follows

$$C_\Omega(q) = \frac{2\pi}{iqu} (\alpha n)^{1-n} \int_{-\frac{(u-i\alpha nq)}{\alpha n}}^{\frac{(u+i\alpha nq)}{\alpha n}} dv \frac{\sinh^n(v)}{v^{n-1}}. \quad (23)$$

Replacing the hyperbolic sine by exponentials and, after expanding the resulting binomial, we can rewrite $C_\Omega(q)$ as follows

$$C_\Omega(q) = \frac{\pi}{iqu} (2\alpha n)^{1-n} \sum_{k=0}^n (-1)^k \binom{n}{k} \int_{-\frac{(u-i\alpha nq)}{\alpha n}}^{\frac{(u+i\alpha nq)}{\alpha n}} dv \frac{\exp[(n-2k)v]}{v^{n-1}}, \quad (24)$$

which is easily calculated in terms of the Incomplete Gamma function.²⁷ The result is

$$C_\Omega(q) = -\frac{2\pi i}{qu} (2\alpha n)^{1-n} \sum_{k=0}^n (-1)^k \binom{n}{k} (2k-n)^{n-2} \operatorname{Im} \left\{ \Gamma \left(2-n, (2k-n) \frac{(u+i\alpha nq)}{\alpha n} \right) \right\}. \quad (25)$$

Going back to $C(q)$, we note that the range of integration can be expanded to all real values of u by adding $C(q)$ to its complex conjugate to get an integrand invariant under the transformation $u \rightarrow -u$. Then, we integrate it by parts to get

$$C(q) = \frac{\alpha\pi^{(3n/2+1)}}{qN} \left(\frac{2}{\alpha n} \right)^{(n/2+1)} \sum_{k=0}^n \binom{n}{k} (-)^k \operatorname{Im} \left\{ \int_{-\infty}^{+\infty} du (u+iq\alpha n)^{1-n} \exp \left[-\frac{u^2}{2\alpha} + \frac{n-2k}{\alpha n} u + iq(n-2k) \right] \right\}. \quad (26)$$

The calculation of the integral in Eq.(26) is straightforward. The result is

$$C(q) = \frac{4\pi^{\frac{3(n+1)}{2}}}{N\alpha^{n-1}n^{\frac{n}{2}+1}} \sum_{k=0}^n \binom{n}{k} (-1)^k \exp \left(\frac{(n-2k)^2}{2\alpha n^2} \right) \operatorname{Re} \left(\exp \left[iq(n-2k) - \frac{i\pi n}{2} \right] U \left(\frac{n-1}{2}, \frac{1}{2}, - \left[\frac{n-2k}{\sqrt{2\alpha n}} + iq n \sqrt{\frac{\alpha}{2}} \right]^2 \right) \right), \quad (27)$$

where $U(a, b, c)$ is Kummer's function²⁷ which can be rewritten in terms of Parabolic Cylinder, Whittaker or other functions. Its mathematical properties like recurrence relations and integral representations are very well known and tabulated.²⁷ But, although its mathemat-

ical properties are many, we were unable to compute the real part in Eq.(27) in a *compact* mathematical form.

Kummer's function has a cut on the negative real axis. Consequently, the evaluation of the norm N and the mean square end-to-end distance $\langle \mathbf{R}^2 \rangle$ cannot be obtained from the Taylor expansion of Eq.(27) in powers of the wave vector \mathbf{q} . Taking into account that both real and imaginary parts of $U(a, b, -|c|)$ have well-known expressions³⁰ we used Eq.(26). Firstly, we interchanged the sum with the imaginary operator and carried out the sum which gives a hyperbolic sine to the n th power. Afterward, the integrand was expanded in powers of the wave vector to third order and the integrals evaluated. The results are

$$N = \frac{(2\pi)^{3n/2+1}}{(\alpha n)^{3n/2-3}} I_{n-2}^n, \quad (28)$$

and

$$\langle \mathbf{R}^2 \rangle = \frac{(2\pi)^{3n/2+1}}{N(\alpha n)^{3n/2-3}} \left\{ (n^2 - n) I_{n-2}^{n-2} - n^2 [2\alpha(n-1) - 1] I_{n-2}^n - (n-1)(n-2) I_n^n \right\}, \quad (29)$$

where

$$\begin{aligned} I_m^p &\equiv \int_{-\infty}^{\infty} dt \frac{\sinh^p(t)}{t^m} \exp \left[-\frac{\alpha n^2}{2} t^2 \right] \\ &= \frac{\sqrt{\pi} n^{m-1} \alpha^{1/2-m/2}}{2^{p+m/2-1/2}} \left\{ -\cos \left(\frac{\pi p}{2} \right) \binom{p}{p/2} \frac{\sqrt{\pi} (-)^{m/2}}{\Gamma(m/2 + 1/2)} \right. \\ &\quad \left. + 2 \sum_{k=0}^{[p/2]} \exp \left[\frac{(p-2k)^2}{2\alpha n^2} \right] \binom{p}{k} (-)^k \operatorname{Re} \left\{ (-i)^m U \left(\frac{m}{2}, \frac{1}{2}, -\frac{(p-2k)^2}{2\alpha n^2} \right) \right\} \right\}. \end{aligned}$$

C. Evaluation of the Polymer Propagator

We now proceed to evaluate the polymer propagator. For this purpose, the starting point is the Fourier transform of the characteristic function given by Eq.(26). Firstly, we

interchange the order of integration as follows

$$P(R) = R^{-1} N^{-1} \frac{\alpha}{2} \pi^{(3n/2-1)} \left(\frac{2}{\alpha n} \right)^{(n/2+1)} \sum_{k=0}^n \binom{n}{k} (-)^k \int_{-\infty}^{+\infty} du \exp \left[-\frac{u^2}{2\alpha} + \frac{n-2k}{\alpha n} t \right] \text{Im} \left\{ \int_0^\infty dq \sin(qR) (u + iq\alpha n)^{1-n} \exp[iq(n-2k)] \right\}, \quad (30)$$

and evaluate the imaginary part of the q -integral assuming that n is even. After replacing $\sin(qR)$ by its definition in terms of exponentials, the propagator can be written in terms of the following integrals

$$W^+(R) = \frac{(-1)^{\frac{n}{2}}}{2(\alpha n)^{n-1}} \text{Im} \left\{ \int_0^{+\infty} dq \frac{\exp(iq(n-2k \pm R))}{(q - iu/\alpha n)^{n-1}} \right\}. \quad (31)$$

which can be solved if we consider q to be a complex variable and apply Cauchy's theorem.

The evaluation of the W -integrals requires special attention to the location of the pole $q = iu/\alpha n$ because u can be positive or negative. For reasons of notation, we define $W_1^+, W_2^+, W_1^-, W_2^-$ such that the subindices 1 and 2 indicate a solution valid for $u \geq 0$ and $u \leq 0$, respectively.

We start by evaluating W^+ using Cauchy's theorem. If $(n-2k+R) \geq 0$, we choose the contour of integration C1 given in Fig. 1. The result for $u \geq 0$ is

$$W_1^+(R) = -\frac{\pi}{2(\alpha n)^{n-1} (n-2)!} \left\{ (n-2k+R)^{n-2} \exp \left[-\frac{t}{\alpha n} (n-2k+R) \right] \right\}. \quad (32)$$

On the other hand, if $u \leq 0$, then $W_2^+(R) = 0$.

The other possibility is $(n-2k+R) \leq 0$. Then, the contour of integration in Fig. 1 should be C2. This implies that $W_1^+(R) = 0$ and

$$W_2^+(R) = \frac{\pi}{2(\alpha n)^{n-1} (n-2)!} \left\{ (n-2k+R)^{n-2} \exp \left[-\frac{t}{\alpha n} (n-2k+R) \right] \right\}. \quad (33)$$

The evaluation of W^- is done in a similar way. If $(n-2k-R) \geq 0$, then the contour of integration should be C1 and the results are $W_2^-(R) = 0$ and $W_1^-(R) = W_1^+(-R)$.

Otherwise, if $(n - 2k - R) \leq 0$, then the contour is C2 and the results are $W_1^-(R) = 0$ and $W_2^-(R) = -W_1^+(-R)$.

Substituting these results into Eq.(30) and evaluating the following integrals

$$\begin{aligned} A_k(R) &\equiv (n - 2k + R)^{n-2} \int_0^{+\infty} dt \exp \left[-\frac{t^2}{2\alpha} - Rt/\alpha Ln \right] \\ &= (n - 2k + R)^{n-2} \sqrt{\pi\alpha/2} \exp \left[R^2/2\alpha n^2 \right] \left[1 - \operatorname{erf} \left(\frac{R}{\sqrt{2\alpha n}} \right) \right], \end{aligned} \quad (34)$$

and

$$\begin{aligned} B_k(R) &\equiv (n - 2k - R)^{n-2} \int_{-\infty}^0 dt \exp \left[-\frac{t^2}{2\alpha} + Rt/\alpha n \right] \\ &= (n - 2k - R)^{n-2} \sqrt{\pi\alpha/2} \exp \left[R^2/2\alpha n^2 \right] \left[1 - \operatorname{erf} \left(\frac{R}{\sqrt{2\alpha n}} \right) \right], \end{aligned} \quad (35)$$

then, the polymer propagator given by Eq.(30) becomes

$$P(R) = \frac{\pi^{(3n/2+1/2)} \alpha^{3(1-n)/2} 2^{n/2+1/2}}{n^{3n/2} (n-2)! N} \exp \left[\frac{R^2}{2\alpha n^2} \right] \sum_{k=0}^{[(n-R)/2]} \binom{n}{k} (-)^k \frac{(n-2k-R)^{n-2}}{R}. \quad (36)$$

This expression, which was obtained assuming that n was even, is easily extended to any number of segments by analytic continuation.

A comparison of this result with the one of the Random Flight Model²³ shows that we can write the final expression for the propagator in a very simple and insightful way

$$P(R) = \frac{\alpha^{3/2} (2\pi)^{(3n/2+3/2)}}{N(\alpha n)^{3n/2}} P_{RFM}(R) \exp \left[\frac{R^2}{2\alpha n^2} \right], \quad (37)$$

where the RMF stands for Random Flight Model.

III. RESULTS AND DISCUSSION

The polymer propagator described by Eq.(37) clearly shows that our treatment of the KP model captures the limit of fully flexible chains ($\alpha \rightarrow \infty$) exactly. Indeed, in this limit, Eq.(37) approaches the well-established expression of the Random Flight Model. Furthermore, Eq.(37) clearly shows how the stiffness of the polymer backbone modifies the propagator of the RFM. In the other limit ($\alpha \rightarrow 0$), the exponential grows. Consequently, those

configurations of the polymer chain with large end-to-end distance have higher probability of been realized than the configurations with small end-to-end distance. This is the correct physical behavior and is a consequence of the free energy penalty related to the formation of hairpins. But, although the exponential function grows in this limit, the propagator of the RFM puts an upper limit to the possible values of the end-to-end distance. This limit is the number of segments of the chain. This is clearly shown in the upper limit of the sum in Eq.(36). Thus, the polymer chain satisfies the local inextensibility constraint. Another very important consequence of Eq.(37) is its mathematical simplicity which makes this expression of the polymer propagator a very good starting point for a perturbative treatment of the KP model as mentioned before.

We plot the normalized radial distribution as a function of the end-to-end distance in Figs. 2, 3, 4 and 5. The values of the parameters chosen are: $n = 6, 10, 20$ and 30 Kuhn segments, and $\alpha = 0.01, 0.02, 0.03, 0.05, 0.1$ and 0.75 . The figures clearly show that the location of the peak in the polymer propagator (multiplied by R^2) moves toward larger values of R when the stiffness of the polymer backbone increases. This behavior is in good qualitative agreement with previous results arising from computer simulation studies¹⁹ and theoretical approaches based on the Maximum Entropy Principle.²⁰ This is the correct result because the stiffer the polymer backbone, the higher the energetic penalty to bend the chain. Consequently, those configurations of the macromolecule with small end-to-end distance will be more and more hindered as the stiffness increases, while those configurations with large end-to-end distance should be more and more favored. Therefore, the peak should shift toward larger values of R when the stiffness increases as shown by the figures.

Figures 6 and 7 show the polymer propagator for polymer chains with 6, 10, 20 and 30 Kuhn segments and a fixed value of the semiflexibility parameter. Theses figures show that the longer the polymer is, the more it behaves like a flexible chain since the location of peak (=end-to-end distance divided by the number of segments) moves toward smaller values. In other words, the longer the polymer is, the less relevant the stiffness of the backbone becomes.

The two aforementioned effects can be easily rationalized in terms of Eq.(37). Observe that the stiffness parameter α and the length of the chain n do not appear as independent variables but, as the product αn^2 . Therefore, making the chain longer is equivalent to increasing the semiflexibility parameter thus making the polymer more flexible.

Another interesting result is the limit of very long chains. It is known that in this limit the polymer propagator of the RFM approaches the one of the Gaussian Chain Model.²⁸ Thus, Eq.(37) should approach the following expression

$$P(R) \sim \exp \left[-\frac{3R^2}{2n} + \frac{R^2}{2\alpha n^2} \right] = \exp \left[-\frac{3R^2}{2n} \left(1 - \frac{1}{3\alpha n} \right) \right] \equiv \exp \left[-\frac{3R^2}{2n (l_K^e)^2} \right], \quad (38)$$

where we have defined an “effective” Kuhn length l_K^e (in units of the bare one, l_K) as follows

$$(l_K^e)^2 = \frac{1}{\left(1 - \frac{1}{3\alpha n} \right)}. \quad (39)$$

Observe that this renormalized Kuhn length approaches the bare one in the limits of very long, $n \rightarrow \infty$, or very flexible chains, $\alpha \rightarrow \infty$. This is the expected result and can be rationalized using the arguments presented in the previous paragraph. In addition, note that as the chain becomes shorter or stiffer, Eq.(39) shows that the effective Kuhn length grows. Therefore, the effects of semiflexibility become more relevant.

Figures 8 and 9 show the behavior of $C(q)$, Eq.(27), as a function of the wave vector q for different values of α and two values of n (10 and 20). The figures clearly show that our treatment of the KP model predicts a smooth transition from the rod-like to the flexible limit. Moreover, our results capture the continuous change in the qualitative behavior of this function which changes from a monotonically decreasing function in the flexible limit to an oscillating function in the rod-like regime. In addition, our computations predict that the decrease of the characteristic function for small values of q should be faster for stiff polymers than for flexible ones. This is a consequence of the fact that rigid polymers have a larger mean squared end-to-end distance than flexible ones for a fixed chain length.

The effect of chain length on the characteristic function is shown in Fig. 10 for the particular cases of chains with 6, 10, 20 and 30 Kuhn segments, and a fixed value of the semiflexibility parameter $\alpha(= 0.01)$. This figure shows that the longer the polymer is, the more it behaves like a flexible chain since the characteristic function approaches the one of a flexible polymer chain.

Figures 11 and 12 show the mean squared end-to-end distance $\langle \mathbf{R}^2 \rangle$ as function of the semiflexibility parameter α for different chain length. Specifically, Fig. 11 compares our

approximate solution, Eq.(29), for $n = 8$ with the exact one.⁵ This figure shows that our approximate solution captures the limits of flexible and rigid polymers exactly and provides an very good behavior in the crossover. Figure 12 shows the behavior of $\langle \mathbf{R}^2 \rangle$ as a function of α for chains with 5, 8, and 10 Kuhn segments.

Finally, we compute the exponent 2ν in the relationship $\langle \mathbf{R}^2 \rangle = n^{2\nu}$. Figure 13 shows the plot of $\ln \{\langle \mathbf{R}^2 \rangle\}$ as function of the number of segments, $\ln(n)$, for two values of the semiflexibility parameter, $\alpha = 0.001$ (rigid) and $\alpha = 0.75$ (flexible). The numerical values of the slopes are 1.95 and 0.98, respectively. These results are in excellent agreement with the expected values for the exponents of rodlike and fully flexible chains. Thus, our approach also captures the fractal dimensions of both limiting behaviors correctly. We have also studied intermediate values of the semiflexibility parameter and observed a smooth crossover from the rod-like to the flexible limit.

IV. CONCLUSIONS

In this paper we have proposed a new treatment of the KP model based on a generating function. The advantage of our approach is two fold. Firstly, the evaluation of the most relevant statistical properties of the model is straight forward since they can be obtained as derivatives or integrals of the generating function. This makes the evaluation of the generating function the crucial step for the solution of the KP model. In our treatment of this model, we were able to devise one approximation that was able to capture the flexible and rigid limits exactly and, moreover, was able to provide a smooth crossover behavior between the two aforementioned limiting regimes. This crossover has all the correct qualitative features as discussed in the previous section. Furthermore, this approximation respects the local, not global, inextensibility constraint. Secondly, our treatment of the KP model was able to provide a good, though not unique, “ground” state around which a perturbative treatment can be developed. We speculate that this perturbative calculation should be able to correct the consequences of our approximation in a systematic and controlled fashion. In other words, this perturbative analysis should account for the corrections arising from the neglected non-local terms in the kernel and deviations of the diagonal terms from the pre-averaging approximation used.

The results presented in the paper are valid for polymers with any number of segments and

value of the stiffness of the polymer backbone. Specifically, we computed the characteristic function, the mean squared end-to-end distance and the polymer propagator of the KP model. Other averages like the radius of gyration and/or correlation functions like the single chain structure factor or tangent-tangent correlation functions can be computed in a straightforward manner, too.

It is worth mentioning that the behaviors predicted for the characteristic function, polymer propagator and mean squared end-to-end distance are in very good qualitative and quantitative agreement with results arising from other studies of the KP and Worm-like Chain Model. This agreement makes us speculate that our future evaluation of the structure factor, the radius of gyration and other correlation functions calculated within the present level of approximation should give good results at least at the qualitative level.

Perhaps, the most important contribution of our work is the derived polymer propagator. The mathematical expression obtained for the propagator is very simple, compact and insightful. It becomes the exact expression of the Random Flight Model in the flexible limit. But, as the stiffness of the polymer backbone increases, the propagator of the RFM is modified by an exponential which depends on the semiflexibility parameter. As a consequence, the peak of the radial distribution function shifts toward larger values of the end-to-end distance when the polymer becomes stiffer. In the limit of infinitely stiff polymers, the propagator becomes a delta function centered at the total contour length of the chain. This is the correct result because the stiffer the polymer backbone, the higher the energetic penalty to bend the chain. This shift of the peak is accompanied by an increase in its height and a decrease in the width of the distribution.

V. ACKNOWLEDGMENTS

We acknowledge the National Science Foundation, Grant # CHE-0132278 (CAREER), the Ohio Board of Regents Action Fund, Proposal # R566 and The University of Akron for financial support.

Appendix A: SOME MATHEMATICAL ASPECTS OF THE EVALUATION OF THE GENERATING FUNCTION

In this appendix we explain how the final expression of the generating function, Eq.(11), was obtained. For the purpose of clarity we define

$$\Upsilon_k \equiv (\Phi_k + i\Psi_{kjp}), \quad (A1)$$

then, the u_k -integrals in Eq.(7) can be evaluated exactly using saddle point which is the solution to the following equations

$$\mathbf{u}_1 - \mathbf{u}_0 = -\kappa \Upsilon_0, \quad (A2)$$

$$\mathbf{u}_{n-1} - \mathbf{u}_{n-2} = \kappa \Upsilon_{n-1}, \quad (A3)$$

$$\mathbf{u}_{k+1} - 2\mathbf{u}_k + \mathbf{u}_{k-1} = -\kappa \Upsilon_k, \quad k = 1..n-2, \quad (A4)$$

where κ was defined in Eq.(12). The solutions to these equations are given by Eq.(9). Moreover, the constraint for the sources, Eq.(10), is a consequence of these equations. Therefore, if this constraint is not satisfied, then Eq. (9) is not the saddle point solution. In addition, those terms appearing in Eq.(7) can be rewritten as follows

$$-\frac{1}{2\kappa} \sum_{k=0}^{n-2} (\mathbf{u}_{k+1} - \mathbf{u}_k)^2 = -\frac{\kappa}{2} \sum_{k=0}^{n-2} \left(\sum_{m=0}^k \Upsilon_m \right)^2, \quad (A5)$$

and also

$$\sum_{k=0}^{n-1} \mathbf{u}_k \cdot \Upsilon_k = -\frac{\kappa}{2} \sum_{k=0}^{n-1} \sum_{m=0}^{n-1} \Upsilon_m |k-m| \Upsilon_k. \quad (A6)$$

We can simplify the sum of these two terms further if we note that

$$\sum_{k=0}^{n-1} \sum_{m=0}^{n-1} \Upsilon_m |k-m| \Upsilon_k + \sum_{k=0}^{n-2} \left(\sum_{m=0}^k \Upsilon_m \right)^2$$

$$= \sum_{k=0}^{n-1} \sum_{m=0}^{n-1} \Upsilon_m |k-m| \Upsilon_k + \sum_{k=0}^{n-2} \sum_{m=0}^k \Upsilon_m \Upsilon_k (n-1-k) + \sum_{k=0}^{n-2} \sum_{m=k+1}^{n-1} \Upsilon_m \Upsilon_k (n-1-m) \quad (\text{A7})$$

$$= \sum_{k=0}^{n-1} \sum_{m=0}^{n-1} \Upsilon_m |k-m| \Upsilon_k - \sum_{k=0}^{n-2} \sum_{m=k+1}^{n-1} \Upsilon_m (m-k) \Upsilon_k + (n-1) \sum_{k=0}^{n-2} \sum_{m=0}^{n-1} \Upsilon_m \Upsilon_k$$

where the last double sum vanishes because of the constraint, Eq.(10). After changing the order of summation we arrive at

$$\sum_{k=0}^{n-1} \sum_{m=0}^{n-1} \Upsilon_m |k-m| \Upsilon_k - \sum_{k=1}^{n-1} \sum_{m=0}^{k-1} \Upsilon_m (k-m) \Upsilon_k. \quad (\text{A8})$$

The first double sum, apart from the term $k=0$, can be separated into two terms. One for $m \leq k-1$ and another one for $m \geq k$ such that the former cancels the second double sum in the previous expression. As a result we obtain

$$\begin{aligned} & \sum_{k=0}^{n-1} \Upsilon_0 k \Upsilon_k + \sum_{k=1}^{n-1} \sum_{m=k}^{n-1} \Upsilon_m |k-m| \Upsilon_k \\ &= \sum_{k=0}^{n-1} \sum_{m=0}^{n-1} \Upsilon_m (m-k) \Theta(m-k) \Upsilon_k. \end{aligned} \quad (\text{A9})$$

If we now use the constraint for the Υ_k 's, Eq.(10), we can readily get the quadratic term in Eq.(11).

References

- ¹G. Porod, *Monatsh. Chem.* **80**, 251 (1949); O. Kratky and G. Porod, *Rec. Trav. Chim.* **68**, 1106 (1949).
- ²N. Saito, K. Takahashi and Y. Yunoki, *J. Phys. Soc. Japan*, **22**, 219 (1967).
- ³H. Yamakawa, *Helical Worm-like Chains in Polymer Solutions* (Springer, Berlin, 1997).
- ⁴H. E. Daniels, *Proc. Roy. Soc. Edinburgh* **A63**, 290 (1952).
- ⁵H. Benoit and P. Doty, *J. Phys. Chem.* **57**, 958 (1953).
- ⁶M. Fixman and J. Kovac, *J. Chem. Phys.* **58**, 1564 (1973).

⁷R. A. Harris and J. E. Hearst, *J. Chem. Phys.* **44**, 2595 (1966).

⁸W. Gobush, H. Yamakawa, W. H. Stockmayer and W. S. Magee, *J. Chem. Phys.* **57**, 2839 (1972).

⁹H. Yamakawa and W. H. Stockmayer, *J. Chem. Phys.* **57**, 2843 (1972).

¹⁰K. F. Freed in *Advances in Chemical Physics*, Vol. 22, Pages 1-128, I. Prigogine and Stuart A. Rice Editors (John Wiley and Sons, New York, 1972).

¹¹M. G. Bawendi and K. F. Freed, *J. Chem. Phys.* **83**, 2491 (1985).

¹²J. B. Lagowski, J. Noolandi and B. Nickel, *J. Chem. Phys.* **95**, 1266 (1991).

¹³R. G. Winkler, P. Reineker and L. Harnau, *J. Chem. Phys.* **101**, 8119 (1994).

¹⁴S. R. Zhao, C. P. Sun and W. X. Zhang, *J. Chem. Phys.* **106**, 2520 (1997).

¹⁵S. M. Bhattacharjee and M. Muthukumar, *J. Chem. Phys.* **86**, 411 (1987).

¹⁶M. G. Poirier *et al.*, *Phys. Rev. Lett.* **86**, **360** (2001); J. F. Leger *et al.*, *Phys. Rev. Lett.* **83**, 1066 (1999); V. Parpura and J. M. Fernandez, *Biophys. J.* **71**, 2356 (1996); M. D. Wang *et al.*, *Biophys. J.* **72**, 1335 (1997); A. D. Mehta, K. A. Pullen and A. Spudich, *FEBS Lett.* **430**, 23 (1998); A. D. Mehta, M. Rief and J. A. Spudich, *J. Biol. Chem.* **274**, 14517 (1999); T. E. Fisher, P. E. Marszalek and J. M. Fernandez, *Nat. Struct. Biol.* **7**, 719 (2000); T. E. Fisher *et al.*, *Trends Biochem. Sci.* **24**, 379 (1999); M. Carrion-Vazquez *et al.*, *Prog. Biophys. Mol. Biol.* **74**, 63 (2000); T. T. Perkins, S. R. Quake, D. E. Smith and S. Chu, *Science* **264**, 822 (1994); S. B. Smith, Y. Cui and C. Bustamante, *Science* **271**, 795 (1996); T. T. Perkins, D. E. Smith and S. Chu, *Science* **276**, 2016 (1997); A. F. Oberhauser, P. E. Marszalek, H. P. Erickson and J. M. Fernandez, *Nature (London)* **393**, 181 (1998); F. Oesterhelt, M. Rief and H. E. Gaub, *New J. Phys.* **1**, 6.1 (1999); H. B. Li, W. K. Zhang, W. Q. Xu and X. Zhang, *Macromolecules* **33**, 465 (2000).

¹⁷J. F. Marko and E. D. Siggia, *Macromolecules* **28**, 8759 (1995); K. Kroy and E. Frey, *Phys. Rev. Lett.* **77**, 306 (1996).

¹⁸P. L. Hansen and R. Podgornik, *J. Chem. Phys.* **114**, 8637 (2001).

¹⁹J. Wilhelm and E. Frey, *Phys. Rev. Lett.* **77**, 2581 (1996).

²⁰R. G. Winkler, *J. Chem. Phys.* **118**, 2919 (2003).

²¹A. L. Kholodenko, *Ann. Phys.* **202**, 186 (1990); A. L. Kholodenko, *J. Chem. Soc. Faraday Trans.* **91**, 2473 (1995); A. L. Kholodenko, *Phys. Lett. A* **141**, 351 (1989); A. L. Kholodenko, *Phys. Lett. A* **178**, 180 (1993); A. Kholodenko and T. Vilgis *Phys. Rev. E* **50**, 1257 (1994); A. L. Kholodenko and T. A. Vilgis *Phys. Rev. E* **52**, 3973 (1995); A. L. Kholodenko, *Macromolecules* **26**, 4179 (1993); A. Kholodenko, M. Ballauff and M. Aguero Granados, *Physica A* **260**, 267 (1998).

²²K. F. Freed, *Renormalization Group Theory of Macromolecules* (John Wiley & Sons, New York, 1987); H. Fujita, *Polymer Solutions* (Elsevier, Amsterdam, 1990); M. Muthukumar and B. G. Nickel, *J. Chem. Phys.* **80**, 5839 (1984); *ibid.* **86**, 460 (1987).

²³M. C. Wang and E. Guth, *J. Chem. Phys.* **20**, 1144 (1952); C. Hsiung, H. Hsiung and A. Gordus, *J. Chem. Phys.* **34**, 535 (1961); M. Marucho and G. A. Carri, *J. Math. Phys.* in press.

²⁴I.S. Gradshteyn and I.M. Ryzhik, *Table of Integrals, Series, and Products* (Academic Press, New York, 2000).

²⁵G. Arfken, *Mathematical Methods for Physicists* (Academic Press, New York, 1985).

²⁶J. Hubbard, *Phys. Rev. Lett.* **3**, 77 (1959); R.D. Strattonovich, *Soviet Phys. Kokl.* **2**, 416 (1958).

²⁷M. Abramowitz and I. Stegun, *Handbook of Mathematical Functions* (Dover, New York, 1970).

²⁸H. Yamakawa, *Modern Theory of Polymer Solutions* (Harper&Row, New York, 1971).

²⁹J. S. Higgins and H. C. Benoit, *Polymers and Neutron Scattering* (Clarendon Press, Oxford, 1996).

³⁰H. Bateman, *Higher Transcendental Functions*, vol. 1 (Mc Graw Hill, New York, 1953) .

List of Figures

- FIG. 1. Contours of integration for the computation of the polymer propagator.
- FIG. 2: Normalized polymer propagator $4\pi R^2 P(R)$ versus R/n for $n = 6$. Continuous line ($\alpha = 0.01$), dashed line ($\alpha = 0.02$), dotted line ($\alpha = 0.03$), dashed-dotted line ($\alpha = 0.05$), dashed-dotted-dotted line ($\alpha = 0.1$) and dashed-dashed-dotted line ($\alpha = 0.75$).
- FIG. 3: Normalized polymer propagator $4\pi R^2 P(R)$ versus R/n for $n = 10$. Continuous line ($\alpha = 0.01$), dashed line ($\alpha = 0.02$), dotted line ($\alpha = 0.03$), dashed-dotted line ($\alpha = 0.05$), dashed-dotted-dotted line ($\alpha = 0.1$) and dashed-dashed-dotted line ($\alpha = 0.75$).
- FIG. 4: Normalized polymer propagator $4\pi R^2 P(R)$ versus R/n for $n = 20$. Continuous line ($\alpha = 0.01$), dashed line ($\alpha = 0.02$), dotted line ($\alpha = 0.03$), dashed-dotted line ($\alpha = 0.05$), dashed-dotted-dotted line ($\alpha = 0.1$) and dashed-dashed-dotted line ($\alpha = 0.75$).
- FIG. 5: Normalized polymer propagator $4\pi R^2 P(R)$ versus R/n for $n = 30$. Continuous line ($\alpha = 0.01$), dashed line ($\alpha = 0.02$), dotted line ($\alpha = 0.03$), dashed-dotted line ($\alpha = 0.05$), dashed-dotted-dotted line ($\alpha = 0.1$) and dashed-dashed-dotted line ($\alpha = 0.75$).
- FIG. 6: Normalized polymer propagator $4\pi R^2 P(R)$ versus R/n for $\alpha = 0.01$. Continuous line ($n = 6$), dotted line ($n = 10$), dashed line ($n = 20$) and dashed-dashed-dotted line ($n = 30$).
- FIG. 7: Normalized polymer propagator $4\pi R^2 P(R)$ versus R/n for $\alpha = 0.1$. Continuous line ($n = 6$), dotted line ($n = 10$), dashed line ($n = 20$) and dashed-dashed-dotted line ($n = 30$).
- FIG. 8: Characteristic function $C(q)$ versus wave vector q for $n = 10$. Dashed-dotted-dotted line ($\alpha = 0$) (the exact solution of rigid Model), dashed-dashed-dotted line ($\alpha = 0.01$), long dashed line ($\alpha = 0.04$), dashed-dotted line ($\alpha = 0.07$), dashed

line ($\alpha = 0.1$), dotted line ($\alpha = 0.75$) and continuous line ($\alpha = \infty$) (the exact solution of the Random Flight Model).

- FIG. 9: Characteristic function $C(q)$ versus wave vector q for $n = 20$. Dashed-dotted-dotted line ($\alpha = 0$) (the exact solution of rigid Model), dashed-dashed-dotted line ($\alpha = 0.01$), long dashed line ($\alpha = 0.04$), dashed-dotted line ($\alpha = 0.07$), dashed line ($\alpha = 0.1$), dotted line ($\alpha = 0.75$) and continuous line ($\alpha = \infty$) (the exact solution of the Random Flight Model).
- FIG. 10: Characteristic function $C(q)$ versus wave vector q for $\alpha = 0.01$. Dotted line ($n = 6$), dashed line ($n = 10$), dashed-dotted line ($n = 20$) and continuous line ($n = 30$).
- FIG. 11: Mean squared end-to-end distance $\langle \mathbf{R}^2 \rangle$ versus the parameter α for $n = 8$. The dotted line is our approximate solution and the dashed line is the exact solution of the KP model[?].
- FIG. 12: Mean square end-to-end distance $\langle \mathbf{R}^2 \rangle$ (in logarithmic scale) versus the parameter α . Dashed-dotted line ($n = 5$), dashed line ($n = 8$) and dotted line ($n = 10$).
- FIG. 13: $\ln \{\langle \mathbf{R}^2 \rangle\}$ versus the number of segments $\ln(n)$. Continuous line ($\alpha = 0.001$) and dashed line ($\alpha = 0.75$).

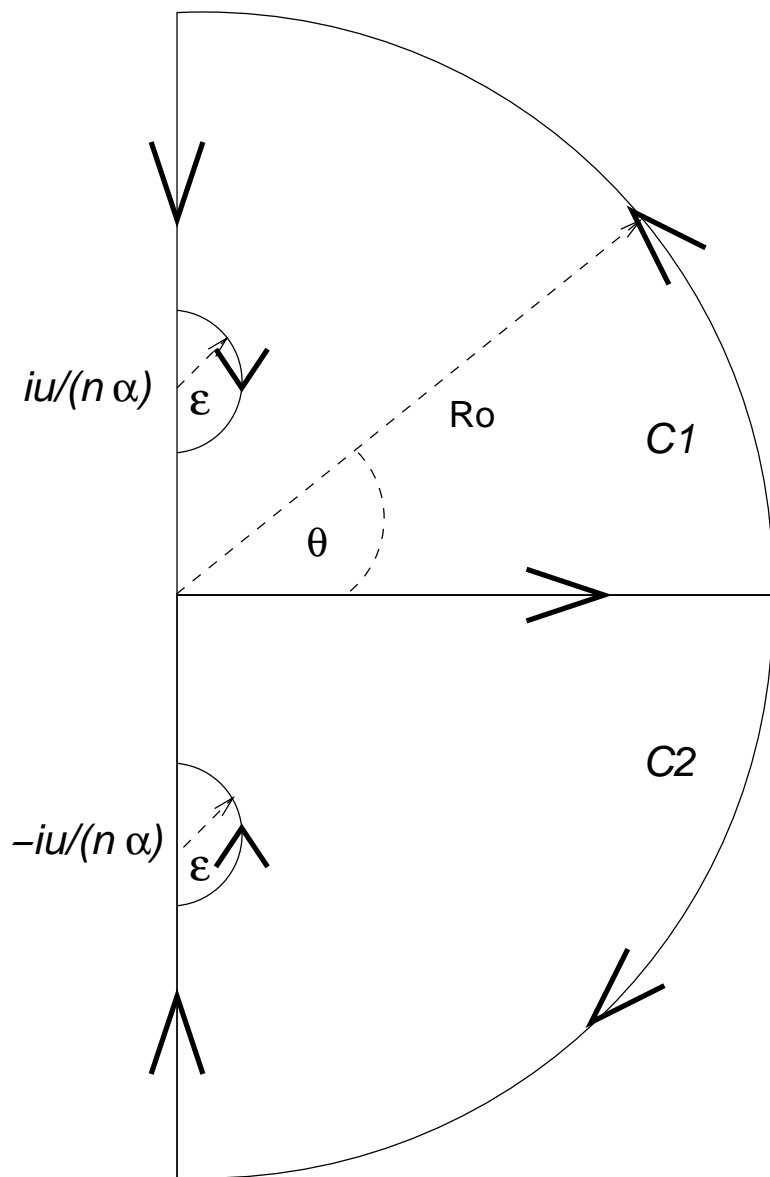


FIG. 1. Contours of integration for the computation of the polymer propagator.

Comment: Figure 1, First Author: Marcelo Marucho, JCP

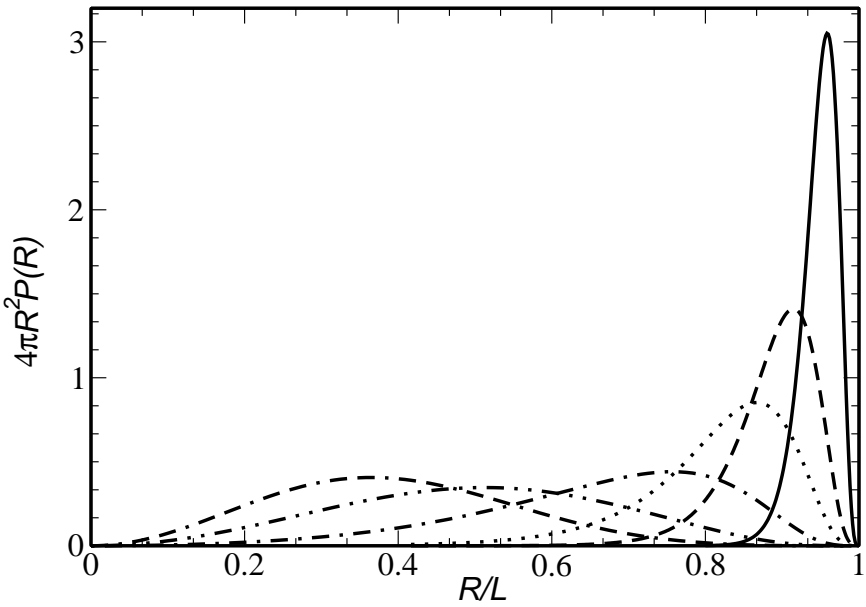


FIG. 2. Normalized polymer propagator $4\pi R^2 P(R)$ versus R/n for $n = 6$. Continuous line ($\alpha = 0.01$), dashed line ($\alpha = 0.02$), dotted line ($\alpha = 0.03$), dashed-dotted line ($\alpha = 0.05$), dashed-dotted-dotted line ($\alpha = 0.1$) and dashed-dash-dotted line ($\alpha = 0.75$).

Comment: Figure 2, First Author: Marcelo Marucho, JCP

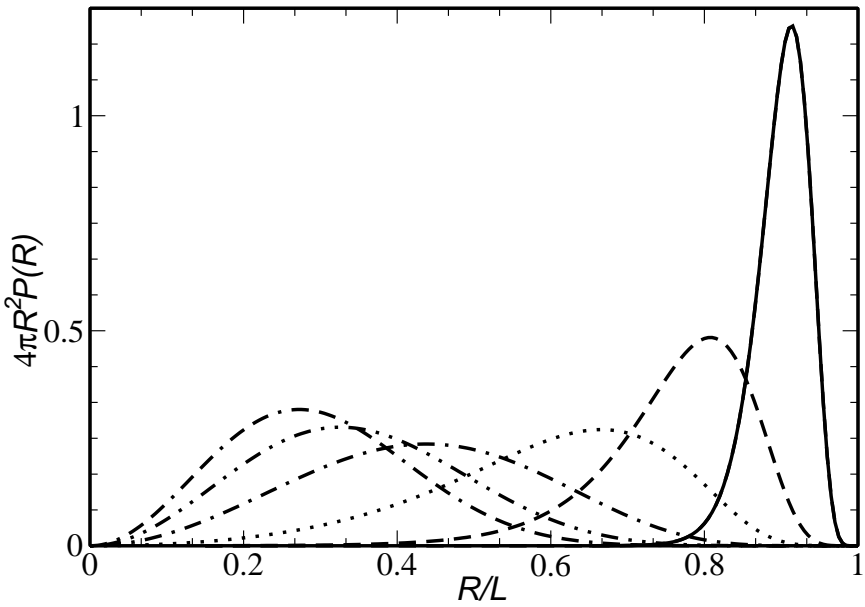


FIG. 3. Normalized polymer propagator $4\pi R^2 P(R)$ versus R/n for $n = 10$. Continuous line ($\alpha = 0.01$), dashed line ($\alpha = 0.02$), dotted line ($\alpha = 0.03$), dashed-dotted line ($\alpha = 0.05$), dashed-dotted-dotted line ($\alpha = 0.1$) and dashed-dashed-dotted line ($\alpha = 0.75$).

Comment: Figure 3, First Author: Marcelo Marucho, JCP

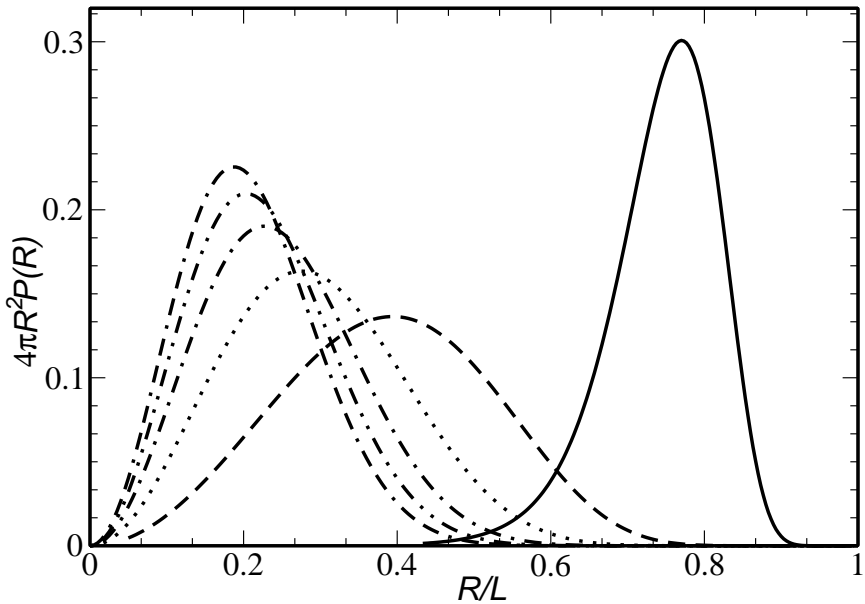


FIG. 4. Normalized polymer propagator $4\pi R^2 P(R)$ versus R/n for $n = 20$. Continuous line ($\alpha = 0.01$), dashed line ($\alpha = 0.02$), dotted line ($\alpha = 0.03$), dashed-dotted line ($\alpha = 0.05$), dashed-dotted-dotted line ($\alpha = 0.1$) and dashed-dashed-dotted line ($\alpha = 0.75$).

Comment: Figure 4, First Author: Marcelo Marucho, JCP

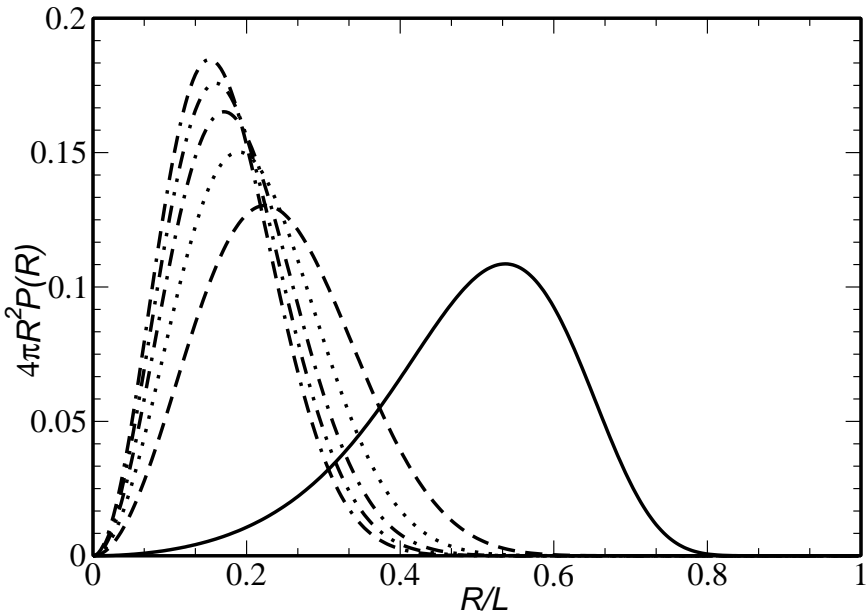


FIG. 5. Normalized polymer propagator $4\pi R^2 P(R)$ versus R/n for $n = 30$. Continuous line ($\alpha = 0.01$), dashed line ($\alpha = 0.02$), dotted line ($\alpha = 0.03$), dashed-dotted line ($\alpha = 0.05$), dashed-dotted-dotted line ($\alpha = 0.1$) and dashed-dashed-dotted line ($\alpha = 0.75$).

Comment: Figure 5, First Author: Marcelo Marucho, JCP

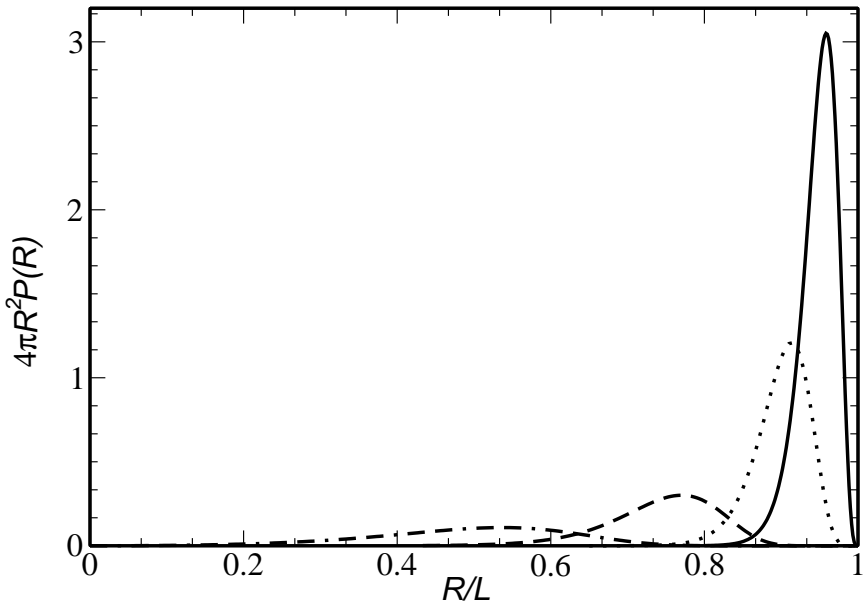


FIG. 6. Normalized polymer propagator $4\pi R^2 P(R)$ versus R/n for $\alpha = 0.01$. Continuous line ($n = 6$), dotted line ($n = 10$), dashed line ($n = 20$) and dashed-dashed-dotted line ($n = 30$).

Comment: Figure 6, First Author: Marcelo Marucho, JCP

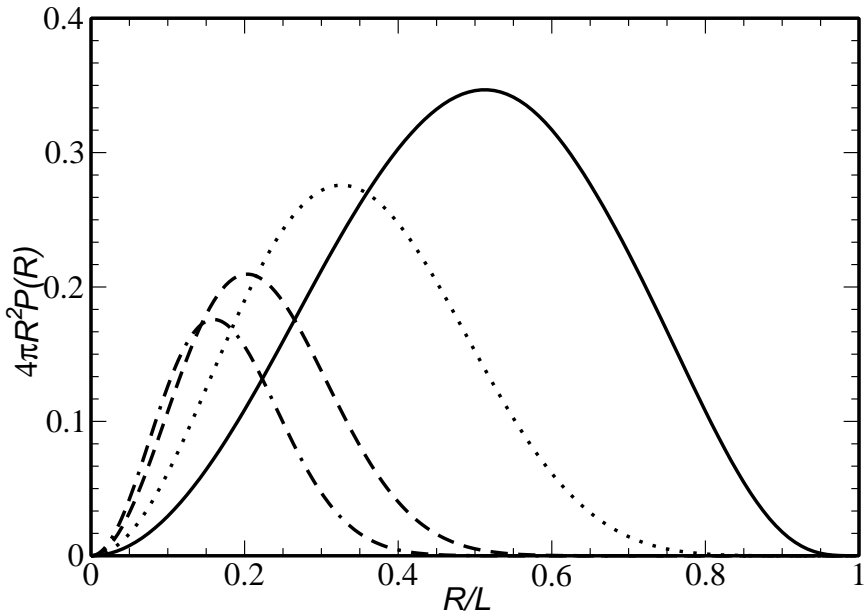


FIG. 7. Normalized polymer propagator $4\pi R^2 P(R)$ versus R/n for $\alpha = 0.1$. Continuous line ($n = 6$), dotted line ($n = 10$), dashed line ($n = 20$) and dashed-dashed-dotted line ($n = 30$).

Comment: Figure 7, First Author: Marcelo Marucho, JCP

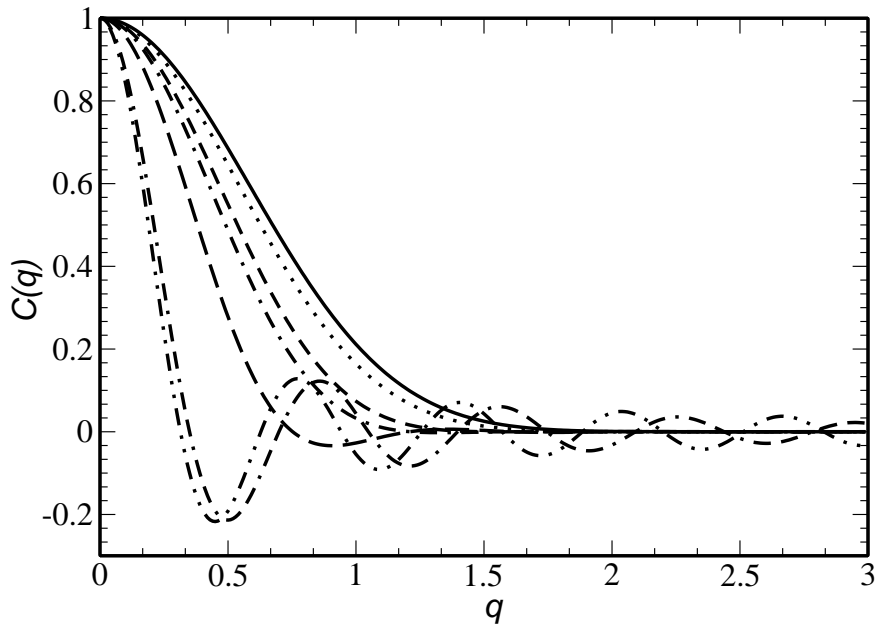


FIG. 8. Characteristic function $C(q)$ versus wave vector q for $n = 10$.
 Dashed-dotted-dotted line ($\alpha = 0$) (the exact solution of rigid Model),
 dashed-dashed-dotted line ($\alpha = 0.01$), long dashed line ($\alpha = 0.04$), dashed-dotted line
 ($\alpha = 0.07$), dashed line ($\alpha = 0.1$), dotted line ($\alpha = 0.75$) and continuous line ($\alpha = \infty$) (the
 exact solution of the Random Flight Model).

Comment: Figure 8, First Author: Marcelo Marucho, JCP

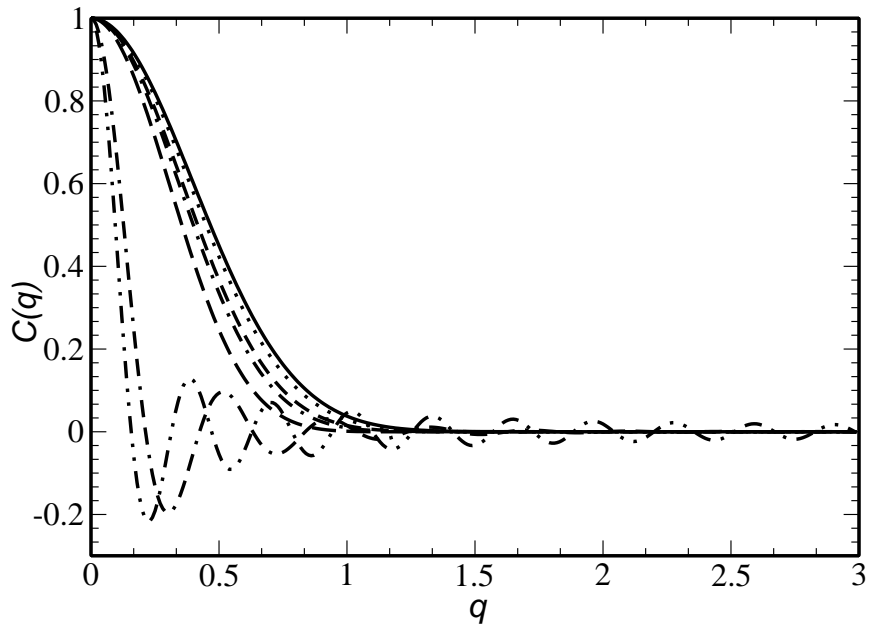


FIG. 9. Characteristic function $C(q)$ versus wave vector q for $n = 20$.
 Dashed-dotted-dotted line ($\alpha = 0$) (the exact solution of rigid Model),
 dashed-dashed-dotted line ($\alpha = 0.01$), long dashed line ($\alpha = 0.04$), dashed-dotted line
 ($\alpha = 0.07$), dashed line ($\alpha = 0.1$), dotted line ($\alpha = 0.75$) and continuous line ($\alpha = \infty$) (the
 exact solution of the Random Flight Model).

Comment: Figure 9, First Author: Marcelo Marucho, JCP

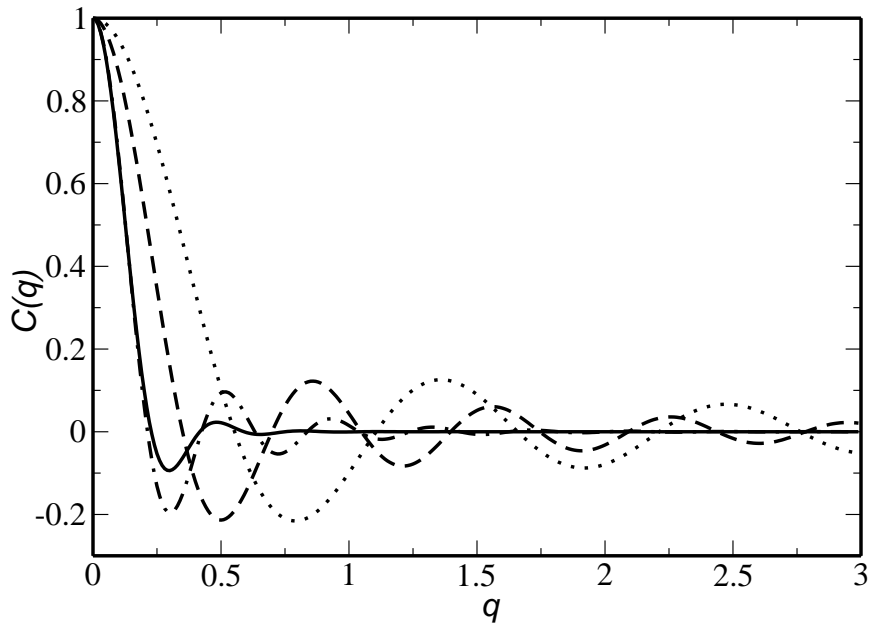


FIG. 10. Characteristic function $C(q)$ versus wave vector q for $\alpha = 0.01$. Dotted line ($n = 6$), dashed line ($n = 10$), dashed-dotted line ($n = 20$) and continuous line ($n = 30$).

Comment: Figure 10, First Author: Marcelo Marucho, JCP

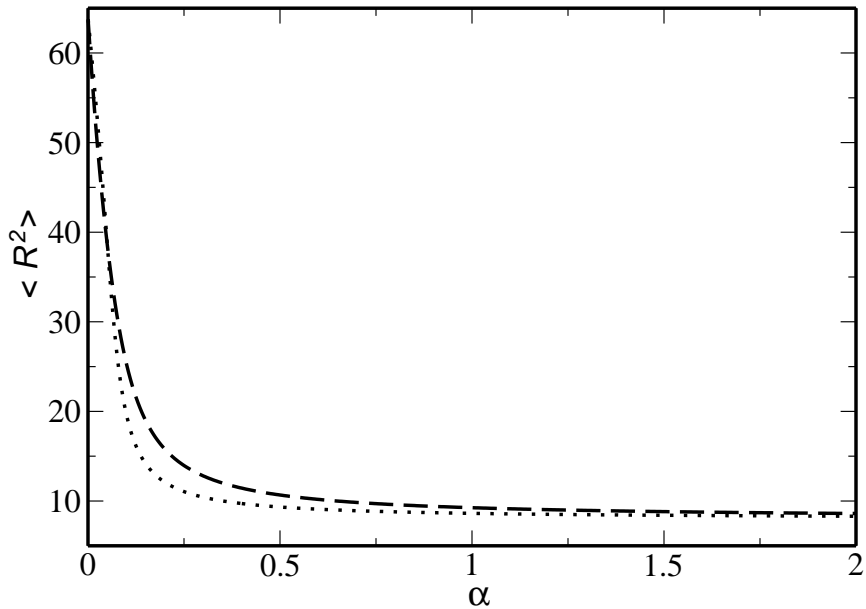


FIG. 11. Mean squared end-to-end distance $\langle \mathbf{R}^2 \rangle$ versus the parameter α for $n = 8$. The dotted line is our approximate solution and the dashed line is the exact solution of the KP model[?].

Comment: Figure 11, First Author: Marcelo Marucho, JCP

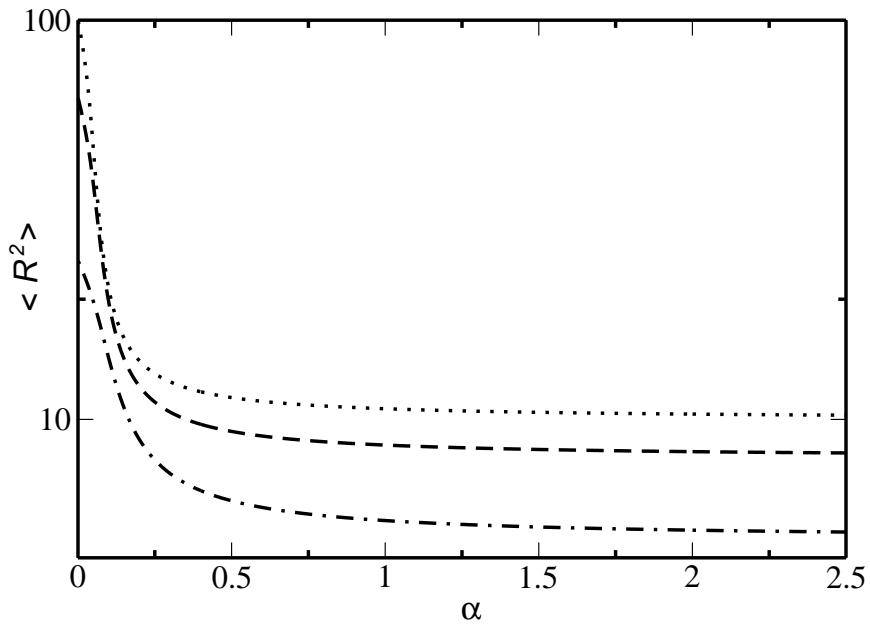


FIG. 12. Mean square end-to-end distance $\langle \mathbf{R}^2 \rangle$ (in logarithmic scale) versus the parameter α . Dashed-dotted line ($n = 5$), dashed line ($n = 8$) and dotted line ($n = 10$).

Comment: Figure 12, First Author: Marcelo Marucho, JCP

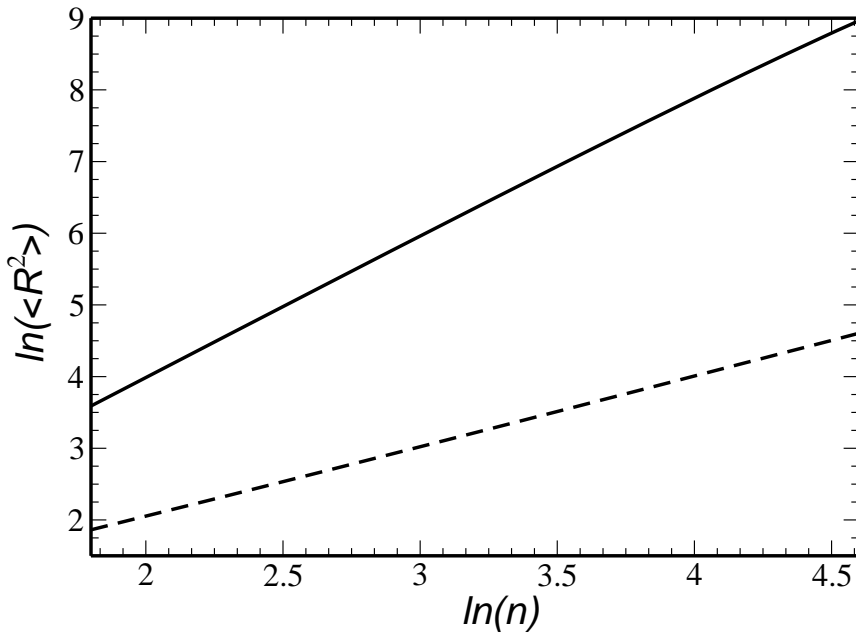


FIG. 13. $\ln \{ \langle \mathbf{R}^2 \rangle \}$ versus the number of segments $\ln(n)$. Continuous line ($\alpha = 0.001$) and dashed line ($\alpha = 0.75$).

Comment: Figure 13, First Author: Marcelo Marucho, JCP